Effect of friction in a toy model of granular compaction

F. Ludewig, S. Dorbolo, and N. Vandewalle
GRASP, Institut de Physique B5, Université de Liège, B-4000 Liège, Belgium
(Received 5 May 2004; published 10 November 2004)

A toy model of granular compaction which includes some resistance due to granular arches is proposed. In this model, the solid/solid friction of contacting grains is a key parameter and a slipping threshold ω_c is defined. Realistic compaction behaviors have been obtained. Two regimes separated by a critical point ω_c^* of the slipping threshold have been emphasized: (i) a slow compaction with lots of paralyzed regions and (ii) an inverse logarithmic dynamics with a power-law scaling of grain mobility. Below the critical point ω_c^*, the physical properties of this frozen system become independent of ω_c. Above the critical point ω_c^*—i.e., for low friction values—the packing properties behave as described by the classical Janssen theory for silos.

DOI: 10.1103/PhysRevE.70.051304 PACS number(s): 45.70.Cc

I. INTRODUCTION

In our industrial world, most of the products are processed, transported, and stocked in their granular state. The density of those granular systems appears therefore to be a crucial parameter for evident economic reasons. In this spirit, the physics of compaction is thus relevant for a broad range of applications [1,2].

Some experimental studies report the evolution of granular packing submitted to successive taps. Experiments on vibrated granular materials exhibit low compaction [3] and phase segregation [4]. In most cases, the density of the material slowly changes as a function of the tap number t and an inverse logarithmic dynamics has been observed. For a few experiments, a fast exponential saturation of the density is obtained [5]. Also, some granular materials may present small density variations (about 1%) from loose packing to dense configurations while, for others, high variations may be observed (up to 20% [6]). Therefore, granular materials exhibit a large diversity of compaction behaviors: according to the taps (reduced acceleration Γ and numbers) and according to the ability to pack (nature and shape of the grains). It is of interest to find out the physical parameters that are relevant for the occurrence of those different compaction dynamics.

In order to reproduce a slow compaction dynamics, the so-called Tetris model has been introduced by Caglioti and co-workers [7]. This toy model considers rectangular blocks placed on a square lattice tilted by 45°. The blocks are submitted to gravity and cannot overlap. At each simulation step, the entire packing is perturbated by a virtual tap in which a number n of motions per grain are realized. During each dynamic step, a grain is moved upward with a probability $p_{up}\left(0<p_{up}<\frac{1}{2}\right)$ and downward with a probability $p_{down}=1-p_{up}$. In the same time, the grain can rotate with a probability $p_{rot}\left(=\frac{1}{2}\right)$. After the dynamical step, the packing relaxes until all grains reach an equilibrium position with respect to gravitation. The main parameter of the Tetris model is the probability ratio $p_{up}/(1-p_{up})$. As a function of this parameter, the acceleration of the taps are tuned and some inverse logarithmic behaviors emerge, for small values. Recently, the Tetris model has shown some relevance for the study of phase segregation occurring in granular binary mixtures [8].

Our main motivation is to propose a simple model which reproduces the behaviors of compaction dynamics and which includes the effect of friction.

II. COMPACTION MODEL

Our toy model is the following. The grains are represented by rectangular blocks, as in the original Tetris model. Two orientations are possible on the tilted lattice. The main rule of this model is a geometrical constraint: two adjacent blocks cannot have the same orientation along the principal axis of the blocks. In so doing, close packing is realized when lines of blocks of one orientation alternate with lines of blocks of the other one—i.e., when the system reaches a quincunx configuration. In this paper, we will refer to this packing as the well-ordered packing or ground state. The potential energy is the lowest. In this state, there is no hole in the structure and a flat top surface.

The initial packing is built using a rain method: the grains are dropped from a random position on the top and stopped when they reach the heap. A loose-packed heap is obtained. A typical configuration is shown in Fig. 1 (top).

In order to take into account the friction, the apparent block weights ω_i are introduced for every block i with a slipping threshold. The weight of a single block ω_b is assumed to be equal to 1 in arbitrary units. Since this calculation is completely deterministic and depends on the block orientations and positions, the contact forces are calculated at each step for every block from top to bottom. The additional rule for including friction is based on a More-Coulomb criterium [9]: when a grain has an apparent weight ω_i larger than a given value ω_c, it cannot move. Figure 1 (right) shows the blocks for which the apparent weights are greater than $\omega_c=12$. This slipping threshold ω_c has a physical relevance. Indeed, the friction force F_i between two grains is given by a certain fraction μ_s of the normal force at the contact. The larger is ω_i, the strongest is the friction force. If a grain has a weight larger than ω_c, the friction is such that it avoids any movement of the grain due to the shock produced by the tap. Thus, the parameter ω_c allows us to tune the amplitude of taps *or* the inverse of the static friction μ_s. Note that the

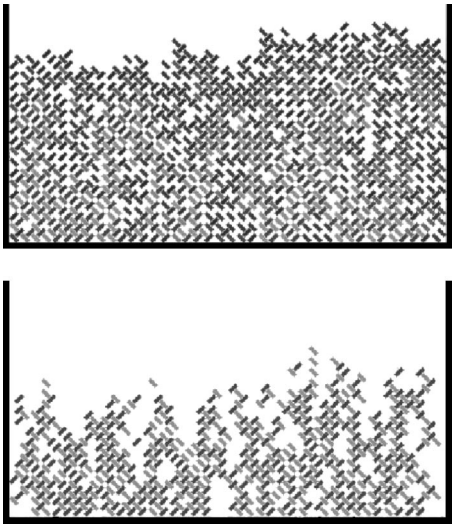

FIG. 1. (Top) Initial configuration of a packing obtained by the "rain" method (see test) for $\omega_c=12$. The gray scale levels emphasize the orientation of the grain. (Bottom) Only grains whose weight is larger than $\omega_c=12$ are represented.

asymptotic value $\omega_c \to \infty$ reduces the model to the Tetris one. On the other hand, a slipping threshold value $\omega_c=1$ leads to a frozen situation—namely, when friction forces are larger than vibration ones (or that the grains are glued together).

In this work, borders have been considered in order to evidence some redirection of the forces towards the walls. The friction between a grain and the border is the same as between two grains.

The rules of a tap simulation are nearly the same as for the original Tetris model. It can be described in two steps: (i) excitation and (ii) relaxation.

(i) A number N of grains are randomly selected. In our simulation, this number N is fixed to the total number of grains lying on the lattice. When the geometry allows it, the grain goes up with a probability p_{up} or goes down with a probability $p_{down}=1-p_{up}$. After grain's translation, if the selected grain has at least three free neighboring sites, it can rotate with a probability $1/2$.

(ii) The entire system is then relaxed. The grains go down until no grain motion is allowed downward. The only one driving force is the gravity.

III. RESULTS

Simulations have been performed for various square lattice sizes from $L=40$ to $L=120$. On such lattices, no jamming is observed. The average total number of particles placed on the lattice with the rain method is equal to two-thirds of the total free sites. The value of $p_{up}/(1-p_{up})$ has been fixed to 1. Changing this parameter will not modify qualitatively the results discussed below.

A. Evolution of the density ρ

The density ρ is evaluated by dividing the total number of the sites by the number of particles in the lowest 25% of the lattice. Figure 2 presents the compacted heap after 10^4 Monte Carlo steps (MCS) taps for a 40×40 lattice. The slipping threshold ω_c has been set to 2, 4, 12, 16, 32, 64 from top to bottom. The situation $\omega_c=2$ is the most constricting one. Indeed, when a block has an upper neighbor, its apparent weight is equal to 2: this block is immediately paralyzed. For a greater value of the slipping threshold ω_c, more grains are free to move. The larger value of ω_c investigated herein is $\omega_c=6400$; it should correspond to a model without friction (like the Tetris one).

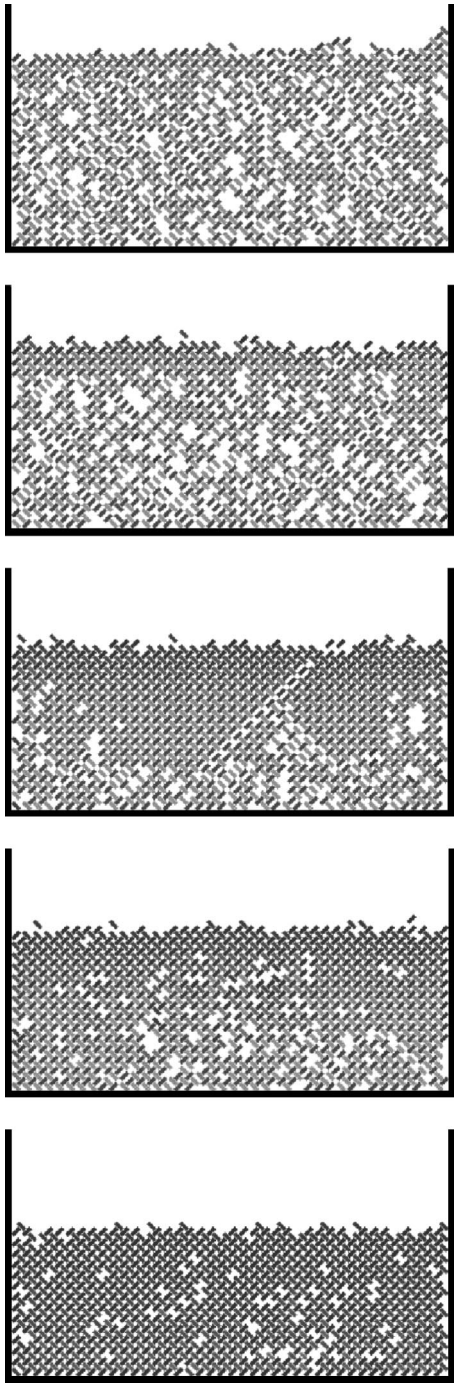

FIG. 2. Simulation of toy model. Six obtained configurations of the heap for different thresholds ω_c after 10^4 MCS taps. From top to bottom: $\omega_c=2$, 4, 12, 16, and 64.

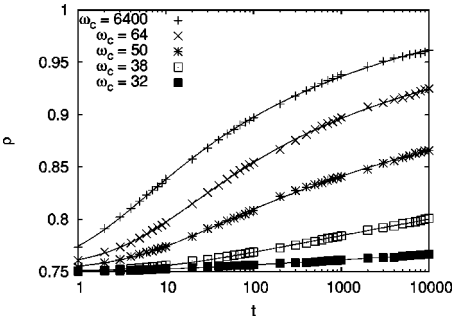

FIG. 3. Evolution of the density ρ with respect to the tap number t in a semilogarithmic plot. The different labels correspond to different slipping threshold ω_c values which are indicated in the legend. From bottom to top, $\omega_c = 32$, 38, 44, 50, 56, 64, and 6400. Simulations have been performed on 100×100 lattices. The solid curves are fits using the inverse logarithmic law, Eq. (1).

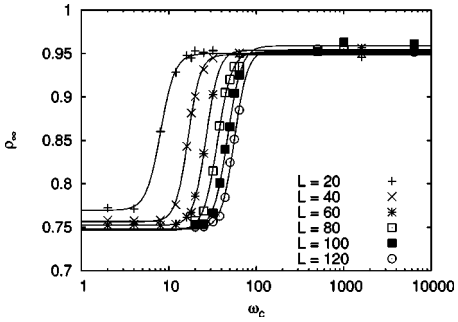

FIG. 4. Semilogarithmic plot of the asymptotic density ρ_∞ as a function of the slipping threshold ω_c for different lattice sizes: $L = 20$, 40, 60, 80, 100, and 120. The solid curves are fitted hyperbolic tangent for determining the critical value ω_c^* of the slipping threshold ω_c.

Two kinds of structures can be seen across the packing: force chains and cavities. The chains of force are defined by the blocks which have a high effective weight. They form lines that propagate through the whole packing. These chains are responsible for the redistribution of the weights in the packing. Moreover, they can lean on the borders; thus a part of the total weight is supported by the borders. Subsequently, some blocks are allowed to support less weight even when they are located near the bottom of the packing. Below the chains of force, caverns may then be found. They are holes in the packing which decrease the global density of the packing because arches resist to the taps.

Caverns are particularly visible in Fig. 2. As ω_c increases, the size of the caverns decreases. Indeed, for large ω_c values, the caverns are reduced to point defects in the "crystalline" quincunx structure. Those defects are very stable, especially when they are located in the bulk of the heap. Among those stable defects, a hole can be surrounded by four blocks which are oriented towards it. Such singularities come from the geometrical laws.

The packing is of course closely linked to the number of these caverns inside the packing. It is noticeable that the number of caverns increases with the considered depth of a packing. In other words, the well-ordered phase *grows* from the top of the packing since the grains are less stressed there. This phenomenon is particularly well seen in Fig. 2 for the particular case $\omega_c = 12$. The notion of cavern is also related to the formation of arches.

The comparison of the heaps after a compaction process shows that the higher ω_c is, the more packed the system becomes. In so doing, the compaction ρ has been plotted with respect to the number of taps in Fig. 3. The graph is represented in a semilogarithmic scale. Several values of the slipping threshold ω_c have been tested and are represented by different symbols (see the legend). The typical evolution of the density is slow during the ten first taps before it drastically increases. A saturation occurs towards a maximum value ρ_∞. The solid curves correspond to fits by a three-parameters law [3,7]

$$\rho(t) = \rho_\infty - \frac{\Delta\rho}{1 + B\ln(1 + t/\tau)}, \tag{1}$$

where ρ_∞ is the asymptotic density when $t \to \infty$, $\Delta\rho$ is the maximum variation of the density, B is a free fitting parameter and t is the number of taps. The parameter τ is a characteristic number of taps. The inverse logarithmic behavior, Eq. (1), is relevant for a slow dynamics of compaction. The complete evolution of ρ can be fitted by this unique law, Eq. (1), for all ω_c values.

The form of Eq. (1) allows us to determine the saturation density ρ_∞ by fitting. The values of ρ_∞ are reported in Fig. 4, with respect to the slipping threshold ω_c. The different curves are obtained for different lattice sizes L: from $L = 20$ up to $L = 120$ lattices. The asymptotic behavior depends on the slipping threshold ω_c: the higher the threshold is, the higher the saturation is. Whatever the size of the lattice, the maximum density ρ_∞ is obtained for high values of the slipping threshold and is equal to approximatively 0.96. A higher density around 1 would have been expected but the presence of the remaining defects are responsible for this difference. An inflection point is found whatever the considered size of the heap. Below this critical point, a poor compaction of the system is observed. Above ω_c^*, compaction of the system takes place. The critical point ω_c^* indicates a change in the compaction dynamics since around that point the asymptotic density may change of 25%. This critical point is shifted towards higher slipping threshold values while the size L of the system is increased.

The inflection point corresponding to the critical slipping threshold ω_c^* has been estimated by fitting a hyperbolic function in a semilogarithmic scale. Figure 5 presents the critical point ω_c^* as a function of the lattice size L. The critical slipping threshold ω_c^* is found to evolve linearily with the lattice size L. According to

$$\omega_c^* \approx 0.43L, \tag{2}$$

as illustrated in Fig. 5. This linear relationship between ω_c^* and L suggests the existence of a characteristic length ξ in the system. This length ξ is thought to be related to the size of the domains of mobile grains. When $\xi < L$, in the packing,

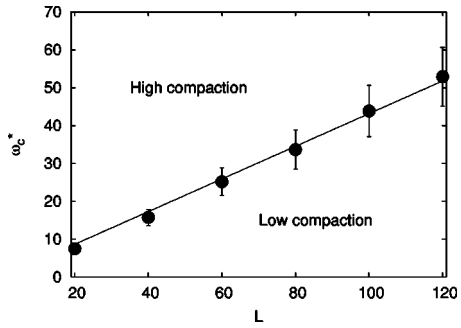

FIG. 5. The critical slipping threshold ω_c^* versus the size L of the lattice. Error bars are indicated. The solid line corresponds to the simple linear fit, Eq. (2).

only a few grains can move freely since most of the grains are frozen by stable arches. Indeed, when this length grows and reaches the system size $L \approx \xi$, arches touch the borders of the lattice. Then, the numerous grains being part of the arches are frozen in that constrained situation. This occurs at the critical point ω_c^*. When $\xi > L$, the entire system is fluid.

There is thus a phase transition at the critical point ω_c^* which depends on the system size. With the linear slip of Fig. 5, the data can be rescaled in order to obtain a unique critical point. This can be seen in Fig. 6. The phenomenon is thus independent of the system size L.

B. Janssen effect

In this paragraph, the ratio of the total weight supported by the borders is calculated. The process that allows the weight to be redirected towards the borders is similar to the one used in the Q model [10]: the grains redistribute their weight to their neighbors below them according to some geometrical rules. In so doing, some stress lines exist and are directed towards the border. Since a friction is considered with the border, a fraction R of the apparent weight is supported by these latter. The fraction R of the apparent weight supported by the border as a function of the slipping threshold ω_c is presented in Fig. 7. If the slipping threshold ω_c is high enough, there is nearly no friction and the grain cannot transmit their apparent weights to the borders.

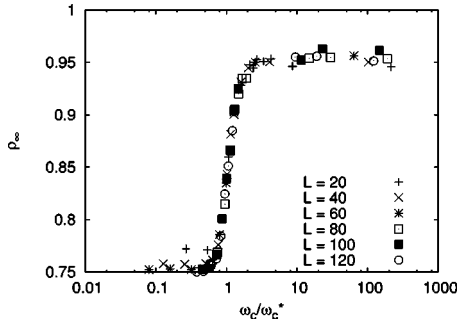

FIG. 6. Semilogarithmic plot of the asymptotic density ρ_∞ as a function of the ratio of slipping threshold ω_c and the critical slipping threshold ω_c^* for different lattice sizes: $L = 20$, 40, 60, 80, 100, and 120.

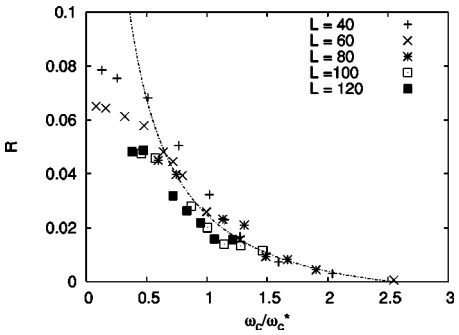

FIG. 7. Evolution of the ratio R of total pile weight ω as a function of the ratio of the slipping threshold ω_c and the critical slipping threshold ω_c^* for different sizes of the lattice L: 20, 40, 60, 80, 100, and 120. The solid curve is a fit with Eq. (5) from $\omega_c/\omega_c^* = 1$ to 3.

In the Janssen theory of silos [9], weights are partially redirected along the horizontal direction. The total pressure P of the packing at the bottom of a silo is given by

$$P = \rho g \chi \left[1 - \exp\left(- \frac{h}{\chi} \right) \right], \tag{3}$$

where the length χ includes the effect of friction along the borders. According to this law, we find

$$\chi = \frac{\chi_0 \omega_c}{\omega_c^*}, \tag{4}$$

where χ_0 is nearly the grain size. The fraction R of lost weight along the borders is given by

$$R = 1 - \frac{\chi_0 \omega_c}{h \omega_c^*} \left[1 - \exp\left(- \frac{h \omega_c^*}{\chi_0 \omega_c} \right) \right], \tag{5}$$

which is valid only when the system is not frustated by small arches—i.e., $\omega_c > \omega_c^*$. The fraction R tends to zero when the friction is zero $(\omega_c \to \infty)$: namely, this corresponds to a fluidlike system. From the data of Fig. 7, we can conclude that our toy model is in agreement with the Janssen theory for $\omega_c > \omega_c^*$. Below the critical point ω_c^*, the physical properties of this frozen system become indepent of ω_c.

C. Grain mobility

According to the previous result that the introduction of the slipping threshold ω_c in a simple compaction model has deep effects when regarding asymptotic densities and pressures in silos. How can we measure the influence of friction on the dynamics of compaction?

The inverse logarithmic dynamics finds its origin in the geometrical constraints of the model. It has been proposed, as for glassy systems, that the mobility μ of the grains decreases during compaction, allowing some trapping of defects in the packing. Power-law scaling has been proposed for the grain mobility μ as a function of $(\rho_\infty - \rho)$. Earlier studies [11,12] have underlined the link between this mobility law and the inverse logarithmic law but the effect of friction has not been studied. We have numerically measured

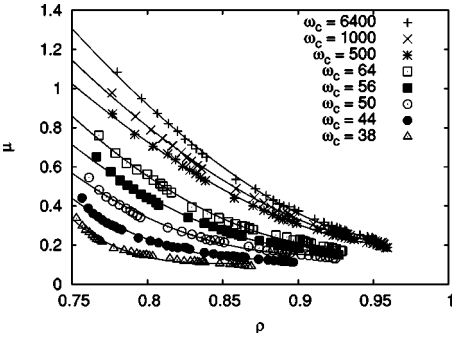

FIG. 8. Grain mobility μ as a function of ρ for different value of the slipping threshold ω_c. The lattice size L is equal to 100.

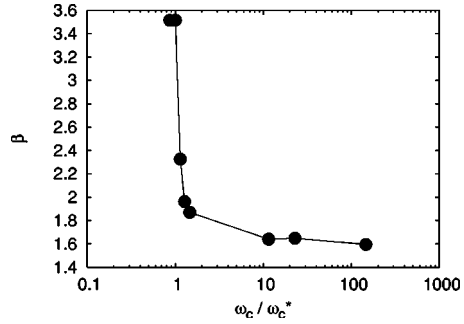

FIG. 9. Evolution of the exponent β as a function of ratio of the slipping threshold ω_c and the critical slipping threshold ω_c^*. The lines conecting data are only a guide for the eye. The lattice size L is equal to 100.

μ in simulations. This quantity μ is measured during each tap. It is the ratio of the moved grains and the total number of grains in the lowest 25% of the lattice. Figure 8 presents a plot of μ as a function of ρ for various values of the slipping threshold ω_c. The power-law scaling

$$\mu = \mu_0 + c(\rho_\infty - \rho)^\beta \tag{6}$$

is found for all data. One should remark that we have considered a residual mobility μ_0 for the free grains in the caverns, the coefficient c being an arbitrary free fitting parameter. The interesting result is that the exponent β of the scaling depends clearly on the friction. Below ω_c^*, the system is frozen and the exponent is close to $\beta \approx 4$. Involving a rapid decrease of the mobility, above ω_c^*; one has, however, a low value $\beta \approx \frac{3}{2}$ involving a slow decrease of the mobility (Fig. 9). This is remarkable that even when the density does not seem to evolve, the grain mobility is still nonzero.

IV. CONCLUSION

Arches have been produced by introducing a slipping threshold ω_c related to the static friction coefficient μ_s between contacting grains. The density has been studied with respect to the number of taps. Two main regimes have been found. For low values of the slipping threshold, the system is completely frozen and the maximum density obtained after tapping is low. For a large value of the threshold ω_c, the system becomes fluid and a clear compaction is possible like in the Tetris model. The transition between both regimes depends on characteristic lengths: some friction length ξ and the system size L.

Above the critical point ω_c*, the model agrees with the Janssen theory of silos. The ratio R of lost weight on the borders vanishes when $\omega_c \to \infty$.

In order to study the dynamics of compaction, we also measured the mobility of the grains. As proposed in earlier studies [11,12], the mobility decreases drastically when ρ reaches the saturation density ρ_∞. A power-law scaling has been found and the mobility exponent β exhibits a large variation above the critical point ω_c^*.

Our work emphasized the revelance of friction on the dynamics of compaction. Experimental studies are needed in order to test those behaviors.

ACKNOWLEDGMENTS

F.L. benefitted from a FRIA grant. S.D. thanks FNRS for financial support. This work is financially supported by ARC Contract No. 02/07-293. We thank H. Caps for fruitful discussions.

[1] H.J. Herrmann, J.P. Hovi, and J.P. Luding, *Physics of Dry Granular Media*, NATO Advanced Study Institute Vol. 350 (Kluwer, Dordrecht, 1998).
[2] R.P. Behringer and J.T. Jenkins, *Powder and Grains* (North-Holland, Rotterdam, 1997).
[3] J.B. Knight, C.G. Fandrich, C.N. Lau, H.M. Jaeger, and S.R. Nagel, Phys. Rev. E **51**, 3957 (1995).
[4] A. Kudrolli, Rep. Prog. Phys. **67**, 209 (2004).
[5] N. Vandewalle and S. Dorbolo, Eur. Phys. J. E **5**, 129 (2001).
[6] G. Lumay and N. Vandewalle (unpublished).
[7] E. Caglioti, V. Loreto, H.J. Herrmann, and M. Nicodemi, Phys. Rev. Lett. **79**, 1575 (1997).
[8] M. Nicodemi, Physica A **285**, 267 (2000).
[9] J. Duran, *Sables, Poudres et Grains* (Eyrolles Sciences, Paris, 1999).
[10] C.-h. Liu, S.R. Nagel, D.A. Schater, S.N. Coppersmith, S. Majumdar, O. Narayan, and T.A. Witten, Science **269**, 513 (1995).
[11] W. Kob and H.C. Andersen, Phys. Rev. E **48**, 4364 (1993).
[12] M. Sellitto and J.J. Arenzon, Phys. Rev. E **62**, 7793 (2000).